Bioconjugate Chemistry

Article

pubs.acs.org/bc

Characterization of Covalent Bond Formation between PPARγ and Oxo-Fatty Acids

Daichi Egawa, Toshimasa Itoh, and Keiko Yamamoto*

Laboratory of Drug Design and Medicinal Chemistry, Showa Pharmaceutical University, 3-3165 Higashi-Tamagawagakuen, Machida, Tokyo 194-8543, Japan

Supporting Information

ABSTRACT: Covalent modification of proteins is important for normal cellular regulation. Here, we report on the covalent modification of peroxisome proliferator-activated receptor γ (PPARγ), an important drug target, by oxo-fatty acids. In this study, ESI mass spectroscopy showed that the reactivities of oxo-fatty acids with PPARγ are different from one another and that these behaviors are related to the structure of the fatty acids. X-ray crystallography showed that three oxo-fatty acids all bound to the same residue of PPARγ (Cys285), but displayed different hydrogen bonding modes. Moreover, fatty acids formed covalent bonds with both PPARγ moieties in the homodimer, one in an active conformation and the other in an alternative conformation. These two conformations may explain why covalently bound fatty acids show partial rather than full agonist activity.

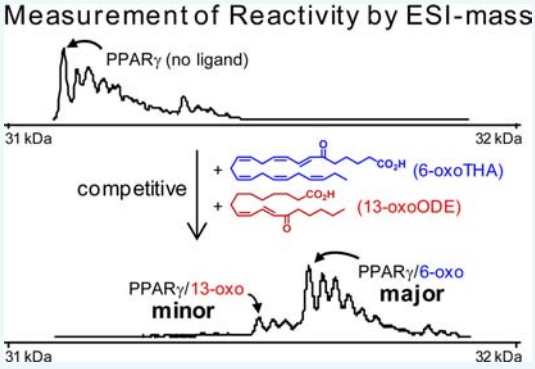

INTRODUCTION

Post-transcriptional protein modification such as phosphorylation,[1] acetylation,[2] ubiquitination,[3] and SUMOylation[4] modulates the structure and thus regulates the function of proteins in important biological events. Covalent protein modification includes modification by lipids, in which Michael addition of protein to lipid occurs. In this reaction the protein acts as a nucleophile while the lipid acts as an electrophile. Covalent modification of protein by lipids makes a substantial contribution to the physiological response under oxidative inflammatory conditions.[5] Since our understanding of protein modification by fatty acids is still fragmented, it is important to use a systematic approach.

Inflammatory conditions create a microenvironment that promotes enzymatic and nonenzymatic oxidation of unsaturated fatty acids to oxo-fatty acids, resulting in an increase in electrophilic fatty acids. Many metabolic and inflammatory events are thought to be regulated by a population of redox-related transcriptional regulatory proteins and enzymes that respond to electrophilic lipid derivatives such as oxo-fatty acids. For example, nuclear factor (erythroid-derived 2)-like 2 (Nrf2) is a well-described redox-dependent transcription factor that plays an important role in the regulation of gene expression related to oxidative and inflammatory injury.[5] Under basal conditions Nrf2 is bound to Kelch-like ECH-associated protein 1 (Keap1); however, when Keap1 is modified by an electrophilic fatty acid (OA-NO_2), a change in its structure leads to the release of Nrf2. This allows Nrf2 to bind the antioxidant response element and activate the expression of phase II genes that code for the antioxidant proteins that remove electrophilic compounds.

Peroxisome proliferator-activated receptor γ (PPARγ) is a nuclear receptor that regulates energy homeostasis events such as fatty acid storage and glucose metabolism. PPARγ is also a redox-dependent transcription factor.[5,6] Several classes of fatty acids have been suggested to be physiologically relevant PPARγ ligands, including prostaglandins, leukotrienes, hydroxy fatty acids, phospholipids, oxo-fatty acids, and nitro fatty acids.[7] However, the functional roles of these classes of fatty acids are unclear. We previously reported that PPARγ covalently binds to oxo-fatty acids.[8] However, details about the covalent bond formation, substrate differences, and resulting biological activity have not been elucidated. In this study we used a chemical approach with PPARγ as a model protein and fatty acids as its covalent modifiers. Here we used X-ray crystallographic analysis and ESI-MASS spectrometry in this systematic study of the binding mode of oxo-fatty acids and their reactions with PPARγ.

RESULTS AND DISCUSSION

Design and Synthesis of Oxo-Fatty Acids. To systematically evaluate the reactivity of oxo-fatty acids with PPARγ, we designed the compounds shown in Figure 1. 4-Oxo-docosahexaenoic acid (4-oxoDHA) **1** and 5-oxo-eicosapentaenoic acid (5-oxoEPA) were synthesized using strategies analogous to those described previously.[9,10] 5-Oxo-tricosahexaenoic acid (5-oxoTrHA) **2** and 6-oxo-tetracosahexaenoic acid (6-oxoTHA) **3** were synthesized from tricosahexaenoic acid

Received: January 9, 2015
Revised: February 28, 2015
Published: March 18, 2015

ACS Publications © 2015 American Chemical Society

DOI: 10.1021/acs.bioconjchem.5b00021
Bioconjugate Chem. 2015, 26, 690−698

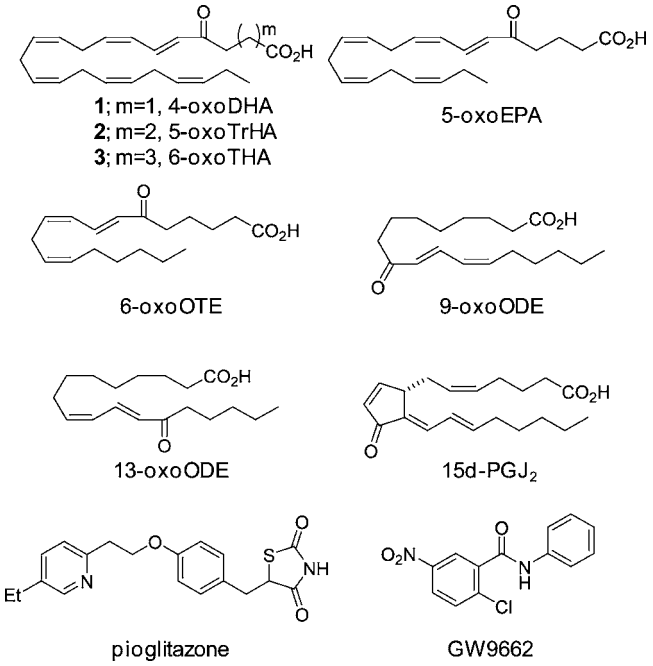

Figure 1. Structures of oxo-fatty acids and PPARγ ligands.

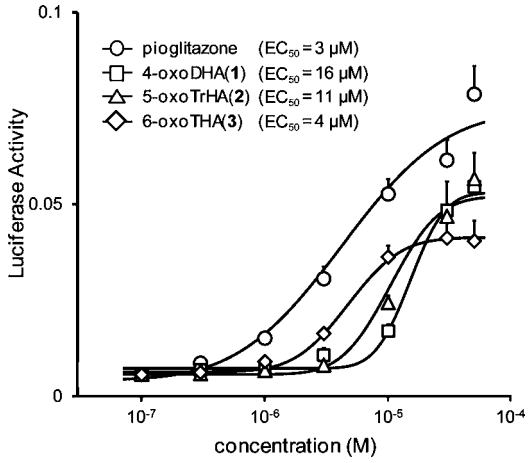

Figure 2. Effect of oxo-fatty acids on PPARγ transcriptional activity. Cos7 cells were transfected with a GAL4-PPARγ chimera expression plasmid (pSG5-GAL-hPPARγ), a reporter plasmid (MH100 × 4-TK-Luc), and an internal control plasmid containing sea pansy luciferase expression constructs (pRL-CMV) and then treated with the indicated oxo-fatty acids or with the PPARγ agonist pioglitazone. Transcriptional activity of PPARγ was evaluated by luciferase activity.

(TrHA) **4** and tetracosahexaenoic acid (THA) **5**, respectively, as shown in Scheme 1. This is the first report of the synthesis of 5-oxoTHA **2** and 6-oxoTrHA **3**. Briefly, TrHA **4** or THA **5** was treated with iodine in the presence of γ-collidine in methylene chloride to afford iodolactone which was then, without purification, treated with DBU in benzene to afford the lactone **6** (47%) or **7** (19%), respectively. The lactone was hydrolyzed in alkaline solution to produce the hydroxyl fatty acid, which was then oxidized by using Dess−Martin periodinane to give 5-oxoTrHA **2** (15%) or 6-oxoTHA **3** (60%).

Cell-Based Assay. Transcriptional activity of PPARγ in 5-oxoTrHA **2** or 6-oxoTHA **3** treated Cos7 cells was evaluated by using a luciferase assay kit. The EC_{50} of 5-oxoTrHA **2** and 6-oxoTHA **3** was 11 μM and 4 μM, respectively (Figure 2). These relatively high EC_{50} values may be due to the oxo-fatty acids trapped by nucleophiles such as GSH in the cytoplasm.[11] The results indicated that both 5-oxoTrHA **2** and 6-oxoTHA **3** are ligands for PPARγ. However, compared to the activity of the full PPARγ agonist pioglitazone in Cos7 cells, the oxo-fatty acids tested here only showed partial agonistic activity (55−70%). It should be noted that PPARγ full agonists used for type 2 diabetes such as thiazolidinediones are related to serious PPARγ-dependent and PPARγ-independent side effects.[12,13] Therefore, development of a partial agonist against PPARγ is an important strategy in the development of type 2 diabetes therapy.

Crystal Structure. To analyze the interactions between the oxo-fatty acids and the PPARγ-ligand binding domain (LBD), we obtained crystals of the PPARγ-LBD/5-oxoTrHA **2** and PPARγ-LBD/6-oxoTHA **3** complexes and solved the crystal structures. We chose co-crystallization to obtain crystals that reflect the reaction in the cell system. Table 1 summarizes the crystallographic data collection and structure refinement statistics for the two structures. The PPARγ-LBD/5-oxoTrHA **2** complex (Figure 3A,B) and the PPARγ-LBD/6-oxoTHA **3** complex (Figure 3C,D) showed quite similar structures; the RMSD of all backbone atoms was measured to be 0.2 Å. These structures are also similar to that of the PPARγ-LBD/4-oxoDHA **1** complex that we previously reported.[8] As shown in Figure 3E, the protein was packed in crystals as a homodimer in which molecule A adopted an active conformation while molecule B adopted an alternative conformation.[14] Helix 12 (magenta) of molecule A folds back to cover the ligand-binding pocket (LBP), while helix 12 (blue) of molecule B binds to the coactivator binding site of molecule A in an adjacent crystal unit (Figure 3E). Thus, two conformers, molecule A and molecule B, are distinct from each other and both conformers are thought to be local minimum structures reflecting protein dynamics in solution. Therefore, we think that the homodimer obtained in this study is valuable and informative.

Figure 4 shows the positioning of the ligands in the LBP of the protein and the interactions between the ligands and the residues. Figure S1 shows the superposition of the simulated annealing composite omit map (CNS, blue) and the refined version of the 2Fo-Fc map (Refmac5, yellow). The ligands (**2** and **3**) were accommodated in both molecules A and B but the positioning and conformation of each ligand in each molecule

Scheme 1

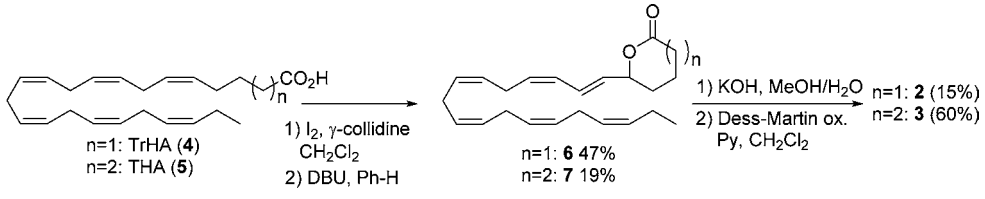

DOI: 10.1021/acs.bioconjchem.5b00021
Bioconjugate Chem. 2015, 26, 690−698

Table 1. Summary of Data Collection Statistics and Refinement of Crystal Structures

ligand	5-oxoTrHA	6-oxoTHA
X-ray source	KEK-PFAR NW-12A	KEK-PFAR NW-12A
Wavelength (Å)	0.97800	0.97800
Space group	*C*2	*C*2
Unit cell dimensions:		
bond (Å)	a = 93.33, b = 61.96, c = 118.79	a = 93.34, b = 61.92, c = 118.82
angle (deg)	α = 90.00, β = 102.86, γ = 90.00	α = 90.00, β = 102.72, γ = 90.00
Resolution range (Å)[a]	36.18−2.30 (2.39−2.30)	40.97−2.40 (2.53−2.40)
Total number of reflections	65160	86740
No. of unique reflections	26806	24200
% completeness[a]	90.7 (85.9)	93.0 (89.7)
R_{merge}[a,b]	0.055 (0.274)	0.074 (0.435)
Refinement statistics:		
Resolution range (Å)[a]	22.93−2.30	33.29−2.40
R factor (R_{free}/R_{work})[a,c]	0.2664/0.2278	0.2788/0.2288

[a]Values in parentheses are for the highest-resolution shell. [b]$R_{merge} = \Sigma|(I_{hkl} - \langle I_{hkl}\rangle)|/(\Sigma I_{hkl})$, where $\langle I_{hkl}\rangle$ is the mean intensity of all reflections equivalent to reflection *hkl*. [c]R_{work} (R_{free}) = $\Sigma||F_{obs}|-|F_{calc}||/\Sigma|F_{obs}|$, where 5% of randomly selected data were used for R_{free}.

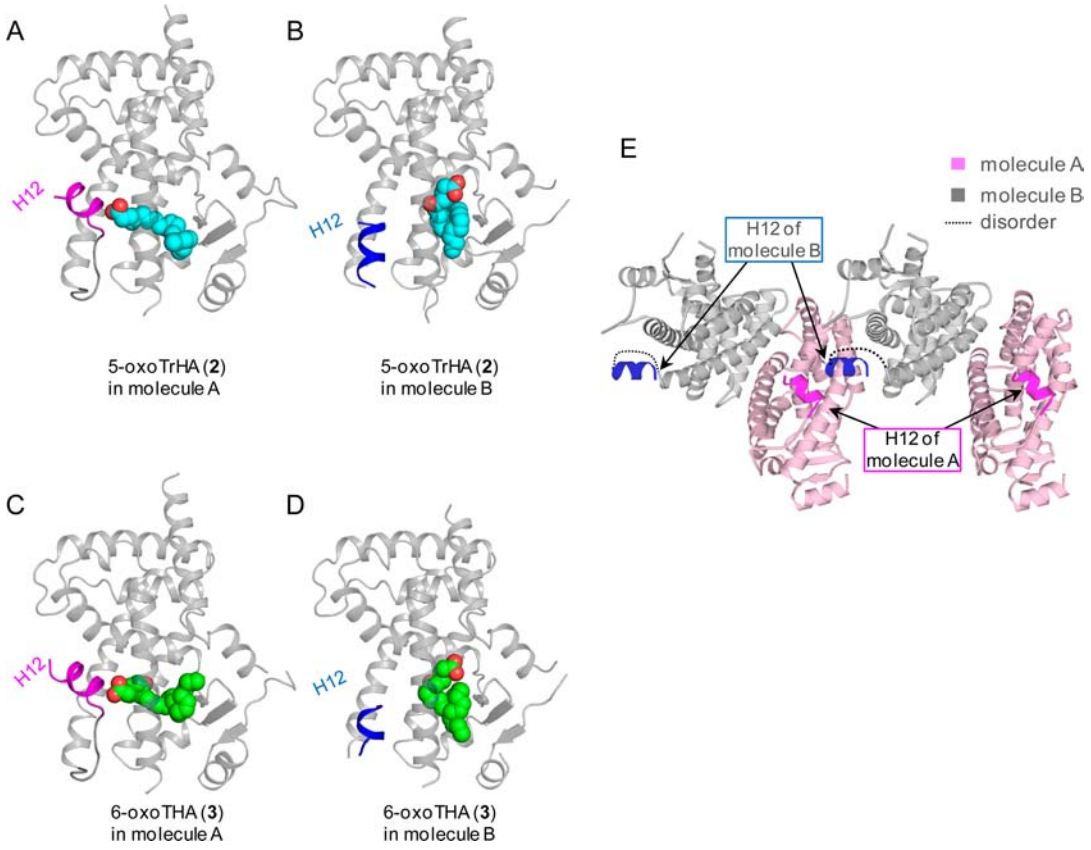

Figure 3. Crystal structures of PPARγ-ligand binding domain (LBD)/oxo-fatty acid complexes and crystal packing. (A) Molecule A shows the active conformation of the PPARγ-LBD/5-oxoTrHA **2** (Cyan) complex. (B) Molecule B shows the alternative conformation of the PPARγ-LBD/5-oxoTrHA **2** (Cyan) complex. (C) Molecule A shows the active conformation of the PPARγ-LBD/6-oxoTHA **3** (Green) complex. (D) Molecule B shows the alternative conformation of the PPARγ-LBD/6-oxoTHA **3** (Green) complex. (E) Crystal packing of PPARγ-LBD/5-oxoTrHA **2** is formed with asymmetric units that contain molecule A (pink) with helix 12 (magenta) folding back to cover the ligand binding pocket (LBP) and molecule B (gray) with helix 12 (blue) binding to the coactivator binding site of molecule A.

were clearly different (Figures 3 and 4). In all complexes, the ligand formed a covalent bond with Cys285 on the LBP. The covalent bond was formed by 1,6-Michael addition of Cys285 to an electrophilic dienone moiety of the fatty acids. Ligands **2** and **3** were accommodated in molecule A in a manner similar to that of 4-oxoDHA **1**. Thus, the carboxylic acid formed hydrogen bonds with Tyr473 in helix 12 and three additional residues (Ser289, His323, and Lys367/His449), and the tail of each ligand extended to the β-sheet side of the LBP. In molecule B, ligands **2** and **3** localized to the β-sheet side of the LBP, with the carboxylic acids of the ligands forming a hydrogen bond with Arg288 at helix 3.

Under the conditions we used, the PPARγ-LBD is known to crystallize as a homodimer in which molecule A and B form

DOI: 10.1021/acs.bioconjchem.5b00021
Bioconjugate Chem. 2015, 26, 690−698

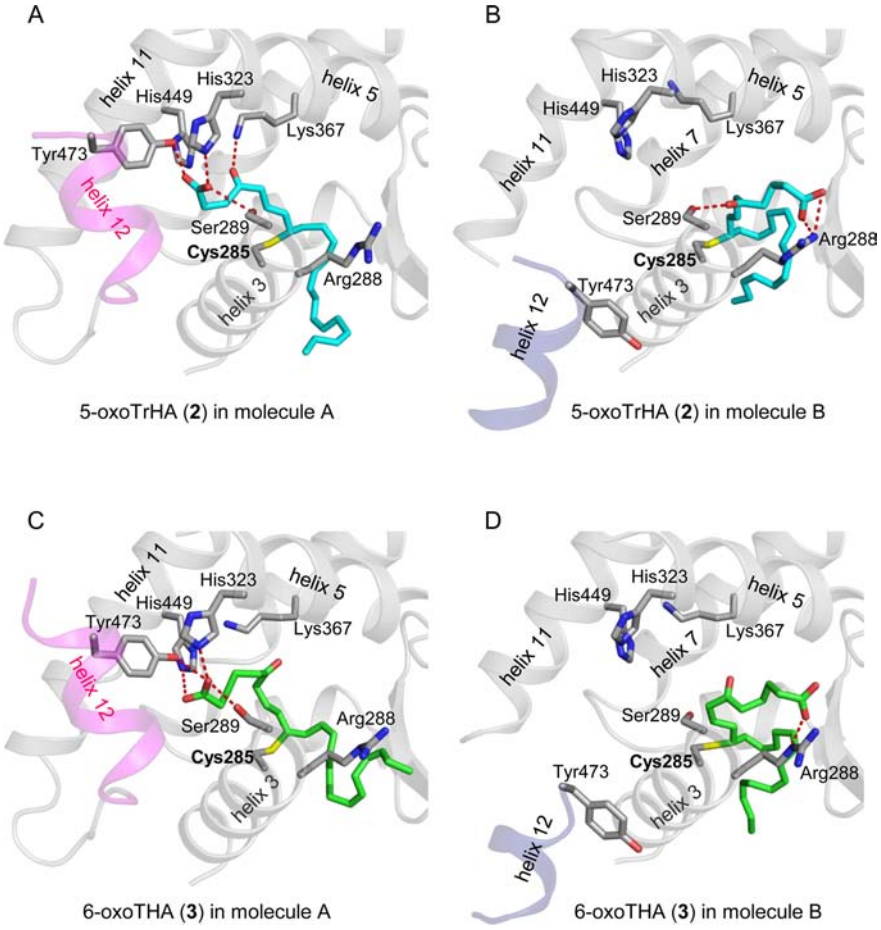

Figure 4. Comparison of the binding conformations of oxo-fatty acids (**2** and **3**) in molecules A and B of the PPARγ-LBD. (A, C) Binding conformation of 5-oxoTrHA **2** (cyan) and 6-oxoTHA **3** (green) in molecule A. These oxo-fatty acids accommodated in molecule A make polar contacts with amino acids including Tyr473 of helix 12. (B, D) The binding conformation of 5-oxoTrHA **2** (cyan) and 6-oxoTHA **3** (green) in molecule B. These oxo-fatty acids accommodated in molecule B make a salt bridge with the Arg288 of helix 3.

active and alternative conformations, respectively. In most cases, synthetic ligands which have polar contact with H12 are contained in molecule A, but there are no ligand in molecule B.[15−25] However, in the present case, the oxo-fatty acids **2** and **3** were accommodated in molecule B of the LBP (Figures 3 and 4). The molecule B conformation observed here is similar to the unliganded molecule B conformations (PDB: 4EMA; RMSD: 0.35 Å).[26] The LBP is large enough to permit the flipping of the carboxylic head of the fatty acid from the Tyr473 side chain to the β-sheet side of the LBP, allowing both conformations of the ligand, one conformation that is characteristic when bound to full agonists and the other characteristic of partial agonists (Figure 4 A-D).

We reanalyzed crystal structures that we reported previously and noticed that oxidized fatty acids that show partial agonist activity for PPARγ were accommodated in molecule B with a similar binding mode as the oxo-fatty acids in the present study, in which the carboxylic acid of the fatty acid and the Arg288 of the LBP formed a salt bridge.[8,14,27] Almost all crystals of PPARγ-LBD/agonist complexes reported so far had been prepared by the ligand soaking method instead of the co-crystallization method that we used. In co-crystallization, almost all PPARγ-LBD proteins immediately accommodate the full agonist to form an active conformation (molecule A), resulting in the lack of alternative conformation (molecule B). Therefore, the crystals of the homodimer consisting of molecule A and molecule B could not be obtained in the presence of a full agonist. Based on the combined data, we propose that this double position of ligands **2** and **3** in the LBP, which stabilizes helix 12 in a different way, may reflect an equilibrium among populations of active and alternative conformations of the PPARγ/fatty acid complex. Similar findings have been demonstrated in interactions between estrogen receptor α and its ligand.[28,29] Quite recently, we have reported similar observations in the crystal structure of a complex of another nuclear receptor; vitamin D receptor (VDR) and its partial agonist showed that the ligand binds to VDR in two conformations, one of which is the agonist/VDR complex structure and the other of which is the antagonist/VDR complex structure.[30] We suggested that the activity of the partial agonist is dependent on the sum of agonistic and antagonistic activities derived from the agonist and antagonist binding conformers, respectively. The two conformations observed here, molecule A and molecule B, may be a similar example that could help explain the partial agonism of ligand-dependent nuclear receptors.

ESI-Mass Spectra. We used ESI-mass spectrometry to confirm the conjugate addition of PPARγ to the various oxo-fatty acids and to compare the electrophilic activity of the fatty acids. First, we used apo-PPARγ-LBD to obtain a good spectrum as shown in Figures 5A and S2. Multiple peaks were observed in this spectrum that were identified as adducts of

DOI: 10.1021/acs.bioconjchem.5b00021
Bioconjugate Chem. 2015, 26, 690−698

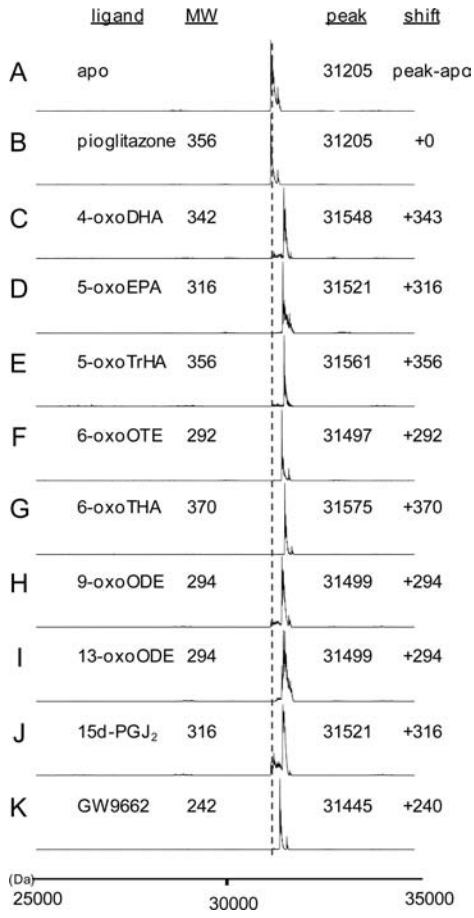

Figure 5. Measurement of reactivity of oxo-fatty acids by ESI-mass spectrometry.

H_2O or Na, or as a molecule with an undigested C-terminal Tyr (Figure S2). Figure 5 shows the ESI-mass spectra of the PPARγ-LBD in the absence and presence of different ligands. In the presence of pioglitazone, the PPARγ-LBD peak showed a 31 205 Da product that corresponded to the molecular weight (MW) of the PPARγ-LBD alone (Figure 5B). For all other compounds, the MW of the PPARγ-LBD increased by the MW of each ligand (Figure 5C−K). This increase in MW of the PPARγ-LBD demonstrated that these ligands covalently bound to PPARγ-LBD. GW9662 has been previously reported to be a covalent binding antagonist of PPARγ.[31] We and another group have reported the covalent binding of 4-oxoDHA **1**, 5-oxoEPA, 6-oxoOTE, 9-oxoODE, 13-oxoODE,[8] and 15d-PGJ_2.[32] Here, we confirm that 5-oxoTrHA **2** and 6-oxoTHA **3** make covalent bonds with PPARγ-LBD (Figure 5E,G).

We next investigated the reactivity of the covalent bond formation between the ligands and the PPARγ-LBD by measurement of the ESI-mass spectra of the PPARγ-LBD following simultaneous incubation with two different ligands for 20 min (Figure 6). Figure 6A shows the spectrum of the PPARγ-LBD incubated in the presence of both 4-oxoDHA **1** and 5-oxoTrHA **2** (black). Both 4-oxoDHA **1** and 5-oxoTrHA **2** adducts were observed but the peaks did not separate. We therefore divided the spectrum into the spectrum of the 4-oxoDHA **1** adduct (red) and that of the 5-oxoTrHA **2** adduct (green) based on a comparison of the original spectrum of the PPARγ-LBD incubated with 4-oxoDHA **1** (Figure 5C) or 5-oxoTrHA **2** (Figure 5E) alone. The ratio of 4-oxoDHA **1** to 5-

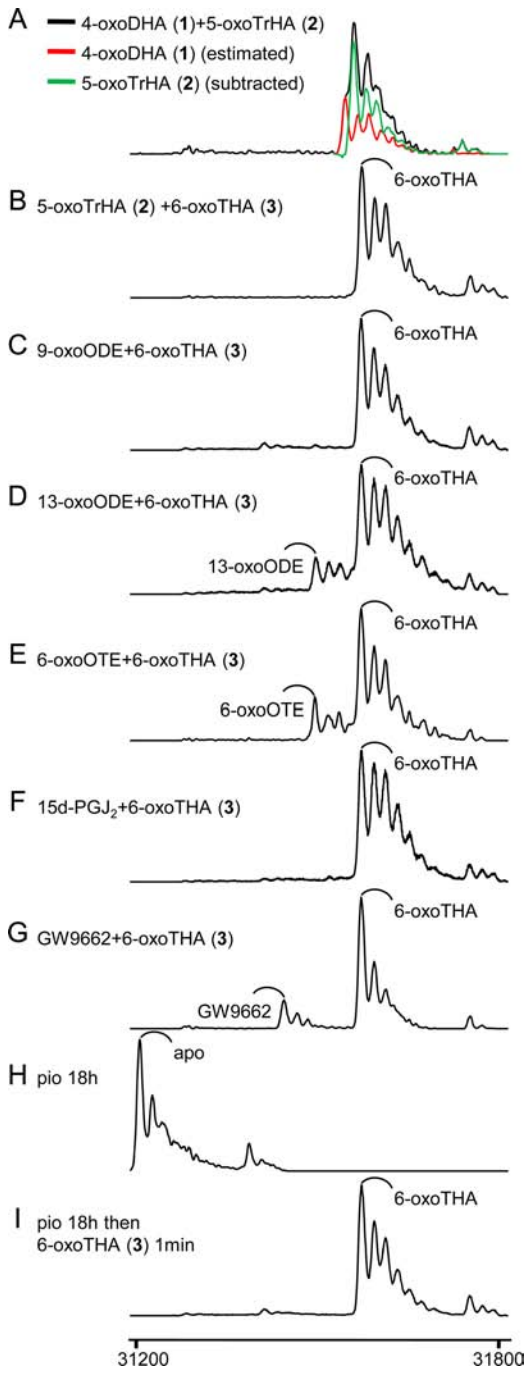

Figure 6. Covalent-binding ability of various oxo-fatty acids to PPARγ-LBD. The reactivity of oxo-fatty acids with the PPARγ-LBD was compared by measuring the ESI mass spectra of the PPARγ-LBD in the presence of two different ligands. (A) 4-oxoDHA **1** vs 5-oxoTrHA **2**. The black line indicates the original spectrum. To separate the peaks of the 4-oxoDHA **1** and 5-oxoTrHA **2** adducts, the original spectrum was divided into the spectrum of the 4-oxoDHA **1** adduct (red) and that of the 5-oxoTrHA **2** adduct (green) based on a comparison of the original spectra of the PPARγ-LBD incubated with 4-oxoDHA **1** (Figure 5C) or 5-oxoTrHA **2** (Figure 5E) alone. The ratio of the 4-oxoDHA **1** adduct (red) and the 5-oxoTrHA **2** adduct (green) was about 2:3. (B) 5-oxoTrHA **2** vs 6-oxoTHA **3**. No peaks corresponding to a 5-oxoTrHA **2** adduct appeared. (C) 9-oxoODE vs 6-oxoTHA **3**. No peaks corresponding to a 9-oxoODE adduct appeared. (D) 13-oxoODE vs 6-oxoTHA **3**. The ratio of 13-oxoODE:6-oxoTHA **3** adducts was about 2:4. (E) 6-oxoOTE vs 6-oxoTHA **3**. The ratio of 6-oxoOTE:6-oxoTHA **3** adducts was about 1:5. (F) 15d-PGJ_2 vs 6-

DOI: 10.1021/acs.bioconjchem.5b00021
Bioconjugate Chem. 2015, 26, 690−698

Figure 6. continued

oxoTHA **3**. No peaks corresponding to a 15d-PGJ_2 adduct appeared. (G) GW9662 vs 6-oxoTHA **3**. The ratio of GW9662 and 6-oxoTHA **3** adducts was about 1:4. (H) Pioglitazone alone. No peaks corresponding to a pioglitazone adduct appeared; only peaks corresponding to apo-PPARγ-LBD were observed. (I) Pioglitazone vs 6-oxoTHA **3**. Pioglitazone was incubated with PPARγ-LBD for 18 h, then 6-oxoTHA **3** was added. The spectrum was measured 1 min after 6-oxoTHA **3** addition. No peaks corresponding to apo-PPARγ-LBD appeared; only peaks corresponding to a 6-oxoTHA **3** adduct were observed.

oxoTrHA **2** adducts was about 2:3, indicating that 5-oxoTrHA **2** is somewhat more reactive than 4-oxoDHA **1**. When PPARγ-LBD was incubated with both 5-oxoTrHA **2** and 6-oxoTHA **3** (Figure 6B), the spectrum showed that only a 6-oxoTHA **3** adduct, not a 5-oxoTrHA **2** adduct, was detected, indicating that 6-oxoTHA **3** is more reactive than 5-oxoTrHA **2** when binding to the LBP (Figure 6B).

A difference of only one carbon between 5-oxoTHA **2** and 6-oxoTrHA **3** significantly changed the reactivity of the fatty acids. This suggests that the flexible region adjacent to the reaction center plays an important role. There are two rigid moieties: one is the carboxylic acid fixed by multiple hydrogen bonds and the other is the dienone moiety composed of sp2 carbons (Figure 7). 4-OxoDHA **1** and 5-oxoTrHA **2** have only two or three carbons between the rigid parts, respectively, while 6-oxoTHA **3** has four. The reaction center, a conjugated olefin, of the less flexible 4-oxoDHA **1** has less of a chance to contact the thiol group of Cys285. In this reaction, the flexibility of 6-oxoTHA **3** appears to be an important feature required for access to the thiol group (Figure 7).

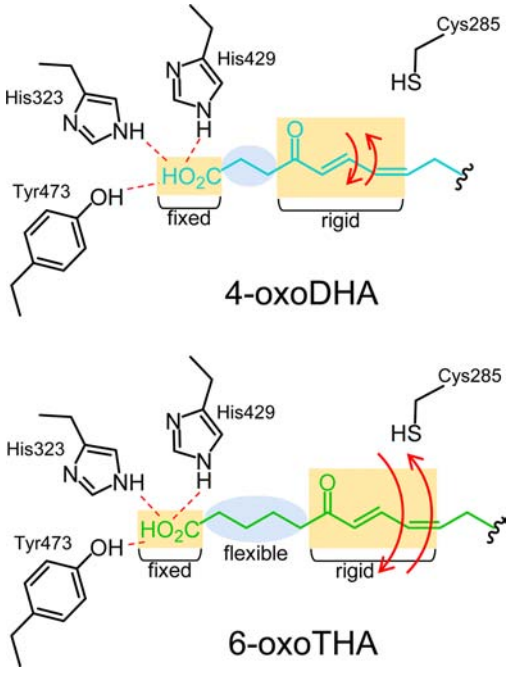

Figure 7. Structure−reactivity relationship of oxo-fatty acids. The range of movement of the reaction center is restricted because of the fixed carbonic acid and rigid conjugated moiety (yellow square). The longer alkyl chain highlighted in pale blue ellipsoid makes the reaction center flexible. Therefore, the conjugated olefin of 6-oxoTHA **3** has a higher probability of being attacked by thiol.

The 9-oxoODE and 13-oxoODE are regioisomers of oxo-linoleic acid that have the same molecular weight. An adduct of 9-oxoODE was not detected when 6-oxoTHA **3** was used as a competitor (Figure 6C). In contrast, an adduct of 13-oxoODE appeared when coincubated with 6-oxoTHA **3**. The adduct ratio of 6-oxoTHA **3**:13-oxoODE was about 4:1 (Figure 6D). These results demonstrated that 6-oxoTHA **3** is a better substrate than either 13-oxoODE or 9-oxoODE and that 13-oxoODE is a better substrate than 9-oxoODE. Even though 9-oxoODE has a longer alkyl chain linking the carboxylic acid and the dienone than that of 6-oxoTHA **3** or 13-oxoODE, 9-oxoODE had the lowest reactivity (Figure S3). This is because the carboxylic acid is fixed on helix 12, and the dienone position of 9-oxoODE is too far from Cys285. This result shows that there is an ideal alkyl chain linking the carboxylic acid and the dienone for optimal PPARγ-LBD binding of oxo-fatty acids.

To further examine the relationship between the total carbon-chain length of the fatty acid and its reactivity with the PPARγ-LBD, we analyzed the ESI spectrum of the PPARγ-LBD that was simultaneously incubated with 6-oxo fatty acids of different carbon chain lengths (Figure 6E). The spectrum showed an adduct ratio of 6-oxoTHA (C24) **3**:6-oxoOTE (C18) of about 3:1, indicating that 6-oxoTHA **3** is a better substrate than 6-oxoOTE. This result suggests that the carbon chain length of the fatty acid affects its reactivity. A hydrophobic pocket might release the less hydrophobic 6-oxoOTE more frequently than 6-oxoTHA **3** before the reaction occurs. This suggests that K_{off}, which is affected by hydrogen bonding with H12 and hydrophobic interactions with the LBP residues, is probably also important for determining the rate of covalent bond formation.

Next, we tested whether this conjugate addition reaction is reversible: 6-oxoTHA **3** was added to the 4-oxoDHA **1** adduct and incubated for 18 h. No peaks corresponding to a 6-oxoTHA **3** adduct were observed; only peaks corresponding to the original 4-oxoDHA **1** adduct were detected (data not shown). This result suggests that the reaction of the conjugate addition to PPARγ is irreversible. The irreversibility of this reaction is perhaps due to the fact that Cys285 is located in the center of the ligand binding pocket, where it is buried within the molecule, and therefore no other molecule can access such a ligand to deprotonate it from the Michael adduct. Consequently, a retro-Michael reaction would not occur unless PPARγ was degraded.

To test the potency of 6-oxoTHA **3** reactivity with PPARγ, 15d-PGJ_2, GW9662, and pioglitazone were used as competitors. 15d-PGJ_2 is known to be a covalent modifier, not only of PPARγ, but also of several other proteins including IκB kinase[33] and eIF4A.[34] GW9662 is a covalent modifier that is an antagonist of PPARγ, and pioglitazone is a noncovalent PPARγ ligand that is widely used as an anti-diabetic drug. When 15d-PGJ_2 was incubated with the PPARγ-LBD together with 6-oxoDHA, only the 6-oxoDHA adduct, and not the 15d-PGJ_2 adduct, was detected (Figure 6F). This result indicated that 15d-PGJ_2 is less potent than several oxo-fatty acids in terms of its reactivity with PPARγ. In the presence of GW9662, although the GW9662 adduct was detected, the adduct ratio of GW9662:6-oxoTHA **3** was 1:4, indicating that 6-oxoTHA **3** is a better substrate for PPARγ than the antagonist GW9662 (Figure 6G). A mixture of pioglitazone (pio) and the PPARγ-LBD showed the same spectrum as that of apo-PPARγ-LBD, indicating that pioglitazone was completely dissociated from the PPARγ-LBD (Figure 6H). This result also indicates that

DOI: 10.1021/acs.bioconjchem.5b00021
Bioconjugate Chem. 2015, 26, 690−698

PPARγ was denatured at the time of detection. Finally, 6-oxoTHA **3** was added to the PPARγ-LBD/pioglitazone mixture, and the mixture was then loaded onto the ESI instrument within 1 min (Figure 6I). A 6-oxoTHA **3** adduct was observed instead of the apo-PPARγ-LBD. This result suggests that pioglitazone in the LBP was rapidly replaced with 6-oxoTHA **3**, and that the electrophilic 6-oxoTHA **3** had completed the formation of a covalent bond with the PPARγ-LBD within 1 min.

Using these approaches, we identified relationships between structure and reactivity of oxo-fatty acids. We call this approach a structure−reactivity relationship (SRR) study. This SRR study is a new way to compare reactivities of biomolecules and may help to probe kinetic parameters of covalent reactivity.

■ CONCLUSION

We have described the characteristics of covalent modification of PPARγ by an oxo-fatty acid using X-ray crystal structure analysis and ESI-mass spectrometry. The results suggest that reactivity during covalent bond formation depends on the structure of the fatty acids. Crystal structures showed that covalently bound fatty acids caused PPARγ to adopt one of two conformations, active and alternative, which may explain the structural basis of partial agonism toward PPARγ. This study contributes not only to our understanding of the physiological roles of covalent modification of proteins but will help inform the design of drugs that can alter covalent modification of target proteins.

■ METHODS

General Experimental Procedures. TrHA and THA were synthesized using docosahexaenoic acid (DHA) ethyl ester according to a previously reported procedure.[35] All other reagents were purchased from commercial sources and were used without further purification. Organic solvents were dried by standard methods. All reactions were performed under a nitrogen atmosphere. Silica gel (Silica Gel 60, spherical, Cica-Reagent) was used for column chromatography, and precoated silica gel 60F254 plates (0.25 mm, Merck) were used for TLC. ^{1}H NMR (300 MHz) and ^{13}C NMR (75 MHz) were recorded in $CDCl_3$ solution with TMS using a Bruker AV300 instrument as an internal standard; the chemical shifts are given in *d* values. Splitting patterns are indicated as follows: s, singlet; d, doublet; t, triplet; q, quartet; quint, quintet; m, multiplet. High resolution mass spectra were obtained using JEOL AccuTOF LC-plus JMS-T100LP and JEOL MS700 spectrometers.

Chemical Synthesis. Experimental details and characterization data for the preparation of 5-oxoTrHA **2** and 6-oxoTHA **3** are provided in the Supporting Information.[35,36]

Transfection and Transactivation Assay. COS-7 cells were cultured in Dulbecco's modified Eagle's medium (DMEM) supplemented with 5% fetal bovine serum (FBS). Cells were seeded on 24-well plates at a density of 2×10^4 per well. After 24 h, a mixture containing 0.18 μg of a reporter plasmid (MH100 × 4-TK-Luc),[37] 0.05 μg of a GAL4-hPPARγ chimera expression plasmid (pSG5-GAL-hPPARγ),[38] 0.02 μg of the internal control plasmid containing sea pansy luciferase expression constructs (pRL-CMV), and 0.75 μL of the Trans IT-LT1 reagent (Mirus, Madison, WI) were added to each well.[39] The MH100 × 4-TK-Luc reporter plasmid contains four copies of the MH100 GAL4 binding site. After 8 h incubation, the cells were treated with either the ligand or ethanol vehicle and were cultured for 16 h. Cells in each well were harvested with a cell lysis buffer, and their luciferase activity was measured using a luciferase assay kit (Promega, WI, USA). Transactivation that was measured as luciferase activity was normalized with the internal control. All experiments were performed in triplicate.

Protein Expression and X-ray Crystallographic Analysis. The human PPARγ-ligand binding domain (LBD) (aa 204−477) was expressed using a modified pET30a vector with an N-terminal 6×His tag cleavable by TEV protease. *E. coli Rosetta* 2 (DE3) was freshly transformed with the plasmid and grown in four flasks containing 0.75 L of 2×TY medium with kanamycin 34 μg/mL and chloramphenicol 50 μg/mL at 37 °C to an OD at 600 nm of 1.0. Protein synthesis was then induced with 0.5 mM isopropyl-β-D-thiogalactopyranoside and the cultures were further incubated at 20 °C for 18 h. Cells were harvested and resuspended in 50 mL lysis buffer (20 mM Tris-HCl pH 8, 100 mM NaCl, 10% v/v Glycerol, 1 mM TCEP, 1 mM AEBSF). Cells were lysed by sonication, and the soluble fraction was isolated by centrifugation (18 000 × *g* for 20 min). The supernatant was applied to Ni-NTA agarose (Qiagen, Santa Clarita, CA) and the resin was thoroughly washed in wash buffer (20 mM Tris-HCl pH 8, 100 mM NaCl, 1 mM TCEP, 1 mM AEBSF). The human PPARγ-LBD was eluted with elution buffer (20 mM Tris-HCl pH 8, 100 mM NaCl, 1 mM TCEP, 1 mM AEBSF, 250 mM imidazole). Turbo TEV protease (25 mg, Accelagen) was added to the eluate and the mixture was incubated at RT for 18 h. The cleaved protein was concentrated in buffer (20 mM Tris-HCl pH 8, 1 mM TCEP, 1 mM AEBSF) and then passed through Ni-NTA agarose. The flow-through was loaded onto a Resource Q (6 mL) column (GE Healthcare) equilibrated with a 20 mM Tris-HCl buffer (pH 7.4). The column was eluted with a NaCl gradient from 0 to 0.5 M (30 mL) in the starting buffer. The eluted fractions were concentrated and loaded onto a Superdex 75 (24 mL) gel-filtration column (GE Healthcare) equilibrated with 20 mM Tris-HCl buffer (pH 7.4). The purified protein was concentrated in buffer (20 mM Tris-HCl pH 8, 0.5 mM EDTA) to a concentration of 8 mg/mL. Protein concentration was estimated by measurement of UV absorbance at 280 nm.

All crystals were obtained by co-crystallization with the relevant ligand. Co-crystallization was performed by vapor diffusion at room temperature using a hanging drop that was made by mixing 1 mL of protein solution (8 mg/mL, in 20 mM Tris-HCl, 0.5 mM EDTA, pH 7.4) with 1 mM ligand in 1 mL of reservoir solution (0.7 M sodium citrate, 0.1 M Tris, pH 8.0 or 7.4) under a nitrogen atmosphere. The mixture was stored in the dark and prismatic crystals (100 to 200 μm) appeared after a few days. Crystals were flash-cooled in liquid nitrogen after a fast soaking in a cryoprotectant buffer (reservoir solution with glycerol 20% v/v). Diffraction data sets were collected at the beamline NW-12A of the Photon Factory Advanced Ring (PF-AR) at the high energy accelerator research organization (KEK) (Tsukuba, Japan). Reflections were recorded with an oscillation range per image of 1.0°. Data were indexed, integrated, and scaled using the MOSFLM[40] and the CCP4[41] suite of programs. The structures were solved using molecular replacement and were rebuilt and refined using COOT,[42] REFMAC,[43] and CNS.[44] At multiple stages, simulated annealing omit maps and simulated annealing composite omit maps (calculated in CNS v 1.2) were used to guide the modeling of the ligand. The coordinate data for the structures were deposited in the Protein Data Bank under the accession

DOI: 10.1021/acs.bioconjchem.5b00021
Bioconjugate Chem. 2015, 26, 690−698

numbers 3X1H (PPARγ-LBD/5-oxoTrHA **2** complex), and 3X1I (PPARγ-LBD/6-oxoTHA **3** complex).

ESI-MASS Spectroscopy. The PPARγ-LBD (500 μL, 2.5 μM) was incubated in 200 μM ammonium acetate buffer with a 4-fold excess of ligand for 0−80 min. All ESI-TOF MS data were collected in an Agilent MSD TOF system. The operating conditions for MS analysis were as follows: positive ion mode, capillary voltage (VCap) 3500 V, nebulizer gas 30 psig, drying gas 5.0 L min^{-1}, fragmentor 140 V, gas temperature 325 °C. The samples were injected into the ion source using a syringe pump (KD Scientific) and a 250 μL Hamilton syringe connected to the ion probe with a 50 μm ID fused silica capillary. The injection flow rate was 10 μL min^{-1}. The averaged MS spectra were deconvoluted using the Agilent MassHunter Workstation Software v B.01.03.

Competitive Reactivity. Mixtures of two different ligands (each 0.5 mM) in 6 μL EtOH were added to 2.5 μM PPARγ-LBD in 200 μM ammonium acetate (294 μL, pH 7.0). The reaction mixtures were kept on ice for 20 min and were then loaded onto an ESI-TOF mass spectroscope at a flow rate of 0.2 mL/min using a syringe pump.

■ ASSOCIATED CONTENT

Ⓢ Supporting Information

Synthesis of oxo-fatty acids **2** and **3** and supporting figures. This material is available free of charge via the Internet at http://pubs.acs.org.

■ AUTHOR INFORMATION

Corresponding Author

*E-mail: yamamoto@ac.shoyaku.ac.jp. Phone: +81 42 721 1580. Fax: +81 42 721 1580.

Notes

The authors declare no competing financial interest.

■ ACKNOWLEDGMENTS

This work was supported by the Platform for Drug Discovery, Informatics, and Structural Life Science and by a Grant-in-Aid for Scientific Research (no. 22790116 and 25860090) from the Ministry of Education, Culture, Sports, Science and Technology, Japan. We also thank the MEXT-Supported Program for the Strategic Research Foundation at Private Universities (2013-2017) and the Takeda Science Foundation, Japan, for financial support. Synchrotron-radiation experiments were performed at the Photon Factory (Proposal No. 2009G647, 2011G685), and we are grateful for the assistance provided by the beamline scientists there.

■ ABBREVIATIONS

PPARγ, peroxisome proliferator-activated receptor γ; Nrf2, nuclear factor (erythroid-derived 2)-like 2; 5-oxoTrHA, 5-oxo-tricosahexaenoic acid; 6-oxoTHA, 6-oxo-tetracosahexaenoic acid; LBD, ligand binding domain; LBP, ligand binding pocket

■ REFERENCES

(1) Johnson, L. N. (2009) The regulation of protein phosphorylation. *Biochem. Soc. Trans. 37*, 627−641.

(2) Choudhary, C., Kumar, C., Gnad, F., Nielsen, M. L., Rehman, M., Walther, T. C., Olsen, J. V., and Mann, M. (2009) Lysine acetylation targets protein complexes and co-regulates major cellular functions. *Science 325*, 834−840.

(3) Bloom, J., Amador, V., Bartolini, F., DeMartino, G., and Pagano, M. (2003) Proteasome-mediated degradation of p21 via N-terminal ubiquitinylation. *Cell 115*, 71−82.

(4) Hay, R. T. (2005) SUMO: a history of modification. *Mol. Cell 18*, 1−12.

(5) Schopfer, F. J., Cipollina, C., and Freeman, B. A. (2011) Formation and signaling actions of electrophilic lipids. *Chem. Rev. 111*, 5997−6021.

(6) Liu, G., Chan, E. C., Higuchi, M., Dusting, G. J., and Jiang, F. (2012) Redox mechanisms in regulation of adipocyte differentiation: beyond a general stress response. *Cells 1*, 976−993.

(7) Nolte, R. T., Wisely, G. B., Westin, S., Cobb, J. E., Lambert, M. H., Kurokawa, R., Rosenfeld, M. G., Willson, T. M., Glass, C. K., and Milburn, M. V. (1998) Ligand binding and co-activator assembly of the peroxisome proliferator-activated receptor-γ. *Nature 395*, 137−143.

(8) Itoh, T., Fairall, L., Amin, K., Inaba, Y., Szanto, A., Balint, B. L., Nagy, L., Yamamoto, K., and Schwabe, J. W. R. (2008) Structural basis for the activation of PPARγ by oxidized fatty acids. *Nat. Struct. Mol. Biol. 15*, 924−931.

(9) Yamamoto, K., Itoh, T., Abe, D., Shimizu, M., Kanda, T., Koyama, T., Nishikawa, M., Tamai, T., Ooizumi, H., and Yamada, S. (2005) Identification of putative metabolites of docosahexaenoic acid as potent PPARγ agonists and antidiabetic agents. *Bioorg. Med. Chem. Lett. 15*, 517−522.

(10) Itoh, T., Murota, I., Yoshikai, K., Yamada, S., and Yamamoto, K. (2006) Synthesis of docosahexaenoic acid derivatives designed as novel PPARγ agonists and antidiabetic agents. *Bioorg. Med. Chem. 14*, 98−108.

(11) Groeger, A. L., Cipollina, C., Cole, M. P., Woodcock, S. R., Bonacci, G., Rudolph, T. K., Rudolph, V., Freeman, B. A., and Schopfer, F. J. (2009) Cyclooxygenase-2 generates anti-inflammatory mediators from omega-3 fatty acids. *Nat. Chem. Biol. 6*, 433−441.

(12) Choi, J. H., Banks, A. S., Estall, J. L., Kajimura, S., Boström, P., Laznik, D., Ruas, J. L., Chalmers, M. J., Kamenecka, T. M., Blüher, M., et al. (2010) Anti-diabetic drugs inhibit obesity-linked phosphorylation of PPARγ by Cdk5. *Nature 466*, 451−456.

(13) Choi, J. H., Banks, A. S., Kamenecka, T. M., Busby, S. A., Chalmers, M. J., Kumar, N., Kuruvilla, D. S., Shin, Y., He, Y., Bruning, J. B., et al. (2011) Antidiabetic actions of a non-agonist PPARγ ligand blocking Cdk5-mediated phosphorylation. *Nature 477*, 477−481.

(14) Einstein, M., Akiyama, T. E., Castriota, G. A., Wang, C. F., McKeever, B., Mosley, R. T., Becker, J. W., M?ller, D. E., Meinke, P. T., Wood, H. B., et al. (2008) The differential interactions of peroxisome proliferator-activated receptor γ ligands with Tyr473 is a physical basis for their unique biological activities. *Mol. Pharmacol. 73*, 62−74.

(15) Pochetti, G., Godio, C., Mitro, N., Caruso, D., Galmozzi, A., Scurati, S., Loiodice, F., Fracchiolla, G., Tortorella, P., Laghezza, A., et al. (2007) Insights into the mechanism of partial agonism: crystal structures of the peroxisome proliferator-activated receptor γ ligand-binding domain in the complex with two enantiomeric ligands. *J. Biol. Chem. 282*, 17314−17324.

(16) Shi, G. Q., Dropinski, J. F., McKeever, B. M., Xu, S., Becker, J. W., Berger, J. P., MacNaul, K. L., Elbrecht, A., Zhou, G., Doebber, T. W., et al. (2005) Design and synthesis of α-aryloxyphenylacetic acid derivatives: a novel class of PPARα/γ dual agonists with potent antihyperglycemic and lipid modulating activity. *J. Med. Chem. 48*, 4457−4468.

(17) Laghezza, A., Pochetti, G., Lavecchia, A., Fracchiolla, G., Faliti, S., Piemontese, L., Di Giovanni, C., Iacobazzi, V., Infantino, V., Montanari, R., et al. (2013) New 2-(aryloxy)-3-phenylpropanoic acids as peroxisome proliferator-activated receptor α/γ dual agonists able to upregulate mitochondrial carnitine shuttle system gene expression. *J. Med. Chem. 56*, 60−72.

(18) Casimiro-Garcia, A., Bigge, C. F., Davis, J. A., Padalino, T., Pulaski, J., Ohren, J. F., McConnell, P., Kane, C. D., Royer, L. J., Stevens, K. A., et al. (2008) Effects of modifications of the linker in a series of phenylpropanoic acid derivatives: Synthesis, evaluation as

DOI: 10.1021/acs.bioconjchem.5b00021
Bioconjugate Chem. 2015, 26, 690−698

PPARα/γ dual agonists, and X-ray crystallographic studies. *Bioorg. Med. Chem. 16*, 4883−4907.
(19) Montanari, R., Saccoccia, F., Scotti, E., Crestani, M., Godio, C., Gilardi, F., Loiodice, F., Fracchiolla, G., Laghezza, A., Tortorella, P., et al. (2008) Crystal structure of the peroxisome proliferator-activated receptor γ (PPARγ) ligand binding domain complexed with a novel partial agonist: a new region of the hydrophobic pocket could be exploited for drug design. *J. Med. Chem. 51*, 7768−7776.
(20) Pinelli, A., Godio, C., Laghezza, A., Mitro, N., Fracchiolla, G., Tortorella, V., Lavecchia, A., Novellino, E., Fruchart, J., Staels, B., et al. (2005) Synthesis, biological evaluation, and molecular modeling investigation of new chiral fibrates with PPARα and PPARγ agonist activity. *J. Med. Chem. 48*, 5509−5519.
(21) Sauerberg, P., Pettersson, I., Jeppesen, L., Bury, P. S., Mogensen, J. P., Wassermann, K., Brand, C. L., Sturis, J., Wöldike, H. F., Fleckner, J., et al. (2002) Novel tricyclic-α-alkyloxyphenylpropionic acids: dual PPARα/γ agonists with hypolipidemic and antidiabetic activity. *J. Med. Chem. 45*, 789−804.
(22) Ohashi, M., Oyama, T., Putranto, E. W., Waku, T., Nobusada, H., Kataoka, K., Matsuno, K., Yashiro, M., Morikawa, K., Huh, N., et al. (2013) Design and synthesis of a series of α-benzyl phenylpropanoic acid-type peroxisome proliferator-activated receptor (PPAR) gamma partial agonists with improved aqueous solubility. *Bioorg. Med. Chem. 21*, 2319−2332.
(23) Kuwabara, N., Oyama, T., Tomioka, D., Ohashi, M., Yanagisawa, J., Shimizu, T., and Miyachi, H. (2012) Peroxisome proliferator-activated receptors (PPARs) have multiple binding points that accommodate ligands in various conformations: phenylpropanoic acid-type PPAR ligands bind to PPAR in different conformations, depending on the subtype. *J. Med. Chem. 55*, 893−902.
(24) Fracchiolla, G., Laghezza, A., Piemontese, L., Tortorella, P., Mazza, F., Montanari, R., Pochetti, G., Lavecchia, A., Novellino, E., Pierno, S., et al. (2009) New 2-aryloxy-3-phenyl-propanoic acids as peroxisome proliferator-activated receptors α/γ dual agonists with improved potency and reduced adverse effects on skeletal muscle function. *J. Med. Chem. 52*, 6382−6393.
(25) Ebdrup, S., Pettersson, I., Rasmussen, H. B., Deussen, H.-J., Frost Jensen, A., Mortensen, S. B., Fleckner, J., Pridal, L., Nygaard, L., and Sauerberg, P. (2003) Synthesis and biological and structural characterization of the dual-acting peroxisome proliferator-activated receptor α/γ agonist ragaglitazar. *J. Med. Chem. 46*, 1306−1317.
(26) Liberato, M. V., Nascimento, A. S., Ayers, S. D., Lin, J. Z., Cvoro, A., Silveira, R. L., Martínez, L., Souza, P. C. T., Saidemberg, D., Deng, T., et al. (2012) Medium chain fatty acids are selective peroxisome proliferator activated receptor (PPAR) γ activators and pan-PPAR partial agonists. *PLoS One 7*, e36297.
(27) Waku, T., Shiraki, T., Oyama, T., and Morikawa, K. (2009) Atomic structure of mutant PPARγ LBD complexed with 15d-PGJ_2: novel modulation mechanism of PPARγ/RXRα function by covalently bound ligands. *FEBS Lett. 583*, 320−324.
(28) Bruning, J. B., Parent, A. A., Gil, G., Zhao, M., Nowak, J., Pace, M. C., Smith, C. L., Afonine, P. V., Adams, P. D., Katzenellenbogen, J. A., et al. (2010) Coupling of receptor conformation and ligand orientation determine graded activity. *Nat. Chem. Biol. 6*, 837−843.
(29) Srinivasan, S., Nwachukwu, J. C., Parent, A. A., Cavett, V., Nowak, J., Hughes, T. S., Kojetin, D. J., Katzenellenbogen, J. A., and Nettles, K. W. (2013) Ligand-binding dynamics rewire cellular signaling via estrogen receptor-α. *Nat. Chem. Biol. 9*, 326−332.
(30) Anami, Y., Itoh, T., Egawa, D., Yoshimoto, N., and Yamamoto, K. (2014) A mixed population of antagonist and agonist binding conformers in a single crystal explains partial agonism against vitamin D receptor: active vitamin D analogues with 22R-alkyl group. *J. Med. Chem. 57*, 4351−4367.
(31) Leesnitzer, L. M., Parks, D. J., Bledsoe, R. K., Cobb, J. E., Collins, J. L., Consler, T. G., Davis, R. G., Hull-Ryde, E. A., Lenhard, J. M., Patel, L., et al. (2002) Functional consequences of cysteine modification in the ligand binding sites of peroxisome proliferator activated receptors by GW9662. *Biochemistry 41*, 6640−6650.
(32) Waku, T., Shiraki, T., Oyama, T., Fujimoto, Y., Maebara, K., Kamiya, N., Jingami, H., and Morikawa, K. (2009) Structural insight into PPARγ activation through covalent modification with endogenous fatty acids. *J. Mol. Biol. 385*, 188−199.
(33) Rossi, A., Kapahi, P., Natoli, G., and Takahashi, T. (2000) Anti-inflammatory cyclopentenone prostaglandins are direct inhibitors of IκB kinase. *Nature 403*, 103−108.
(34) Kim, W. J., Kim, J. H., and Jang, S. K. (2007) Anti-inflammatory lipid mediator 15d-PGJ_2 inhibits translation through inactivation of eIF4A. *EMBO J. 26*, 5020−5032.
(35) Itoh, T., Tomiyasu, A., and Yamamoto, K. (2011) Efficient synthesis of the very-long-chain n-3 fatty acids, tetracosahexaenoic acid (C_{24}:6n-3) and tricosahexaenoic acid (C_{23}:6n-3). *Lipids 46*, 455−461.
(36) Itoh, T., Yoshimoto, N., and Yamamoto, K. (2010) Synthesis of oxidized fatty acid derivatives via an iodolactonization reaction. *Heterocycles 80*, 689−695.
(37) Kang, T., Martins, T., and Sadowski, I. (1993) Wild type GAL4 binds cooperatively to the GAL1−10 UAS_G in vitro. *J. Biol. Chem. 268*, 9629−9635.
(38) Lehmann, J. M., Moore, L. B., Smith-Oliver, T. A., Wilkison, W. O., Willson, T. M., and Kliewer, S. A. (1995) An antidiabetic thiazolidinedione is a high affinity ligand for peroxisome proliferator-activated receptor γ (PPARγ). *J. Biol. Chem. 270*, 12953−12956.
(39) Yamamoto, K., Masuno, H., Choi, M., Nakashima, K., Taga, T., Ooizumi, H., Umesono, K., Sicinska, W., VanHooke, J., DeLuca, H. F., et al. (2000) Three-dimensional modeling of and ligand docking to vitamin D receptor ligand binding domain. *Proc. Natl. Acad. Sci. U. S. A. 97*, 1467−1472.
(40) Leslie, A. G. W. (2006) The integration of macromolecular diffraction data. *Acta Crystallogr., Sect. D: Biol. Crystallogr. 62*, 48−57.
(41) Collaborative Computational Project Number 4. (1994) The CCP4 suite: programs for protein crystallography. *Acta Crystallogr., Sect. D: Biol. Crystallogr. 50*, 760−763.
(42) Emsley, P., and Cowtan, K. (2004) Coot: model-building tools for molecular graphics. *Acta Crystallogr., Sect. D: Biol. Crystallogr. 60*, 2126−2132.
(43) Murshudov, G. N., Vagin, A. A., and Dodson, E. J. (1997) Refinement of macromolecular structures by the maximum-likelihood method. *Acta Crystallogr., Sect. D: Biol. Crystallogr. 53*, 240−255.
(44) Brunger, A. T. (2007) Version 1.2 of the crystallography and NMR system. *Nat. Protoc. 2*, 2728−2733.

DOI: 10.1021/acs.bioconjchem.5b00021
Bioconjugate Chem. 2015, 26, 690−698